

Military Technical College
Kobry El-Kobbah,
Cairo, Egypt.



15th International Conference
on Applied Mechanics and
Mechanical Engineering.

KRYLOV-BOGOLIUBOV APPROACH TO NON-LINEAR HYSTERETIC INSTABILITY IN ROTORDYNAMICS

F. Sorge^{*}

ABSTRACT

The internal friction due to the shaft hysteresis or the shrink fitting release exerts a destabilizing effect on the overcritical rotor whirl, but may be counteracted by other external dissipative sources and/or by proper anisotropy of the support stiffness. The internal friction effect may be treated by either dry or viscous models, obtaining similar results in the hypothesis of small dissipation levels, provided that proper equivalence criteria are defined between the two approaches. The equivalence is here stated by imposing the same energy dissipation over a large number of shaft revolutions. Approximate closed-form autonomous solutions for a symmetric rotor arrangement subject to Coulombian non-linear friction are derived by an averaging approach of the Krylov-Bogoliubov type, in order to ascertain the result similarity between the two dissipative assumptions. Summing up, the viscous equivalent linear assumption appears conservative in general and may be accepted for a straightforward analysis of the overall rotor dynamics in the whole speed range.

KEYWORDS

Conical Rotor Whirl, Hysteresis, Stability, Averaging Techniques.

^{*} Professor, DICGIM, University of Palermo, Italy.

INTRODUCTION

As well known, the internal friction may exert a destabilizing influence in the speed range above the first critical speed, whose consequences may be important if the hysteretic properties of the material are remarkable (e. g. carbon/epoxy [1]). In despite of this, the unstable trend can be efficiently counterbalanced by other external dissipative sources. For example, suspending the journal boxes and letting them rub against dry friction surfaces on the frame, a strong damping action can be achieved, together with an excellent contrast to the critical flexural speeds [2-5].

The first approaches to this problem date from references [6-8]. Reference [9] reports a valuable stability analysis for a symmetric rotor on a hysteretic shaft, where the stability threshold is searched by the Routh-Hurwitz criterion. More recent analyses develop in-depth formulations, where the system asymmetry, the gyroscopic effects and the anisotropy of the supports are taken into consideration [10-14]. Other papers focus on the particular damping properties of the supports, for example hydrostatic bearings or optimized viscoelastic suspensions [15-16]. Approaches in terms of finite elements are also widely present in literature, together with thorough treatises covering several aspects [17-20].

The present analysis firstly develops the preliminary results of reference [21], addressing the conical whirling motions of an asymmetric unbalanced rotor-support assembly subject to different suspension stiffness and damping coefficients in the horizontal and vertical planes. The natural frequencies are traced on Campbell diagrams, the elliptical paths of the rotor and the bearings are calculated in the speed range and the stability of the steady motion is checked by the Routh-Hurwitz procedure in dependence on the gyro structure, on the support anisotropy and on the system asymmetry, showing how the hysteretic instability can be conveniently prevented by differentiating the suspension stiffness in two orthogonal inflexion planes. Wide-ranging numerical solutions indicate that the viscous linear hypothesis gives conservative instability thresholds in comparison with the Coulombian assumption when the equivalence is based on the same energy dissipation over a large number of shaft revolutions.

Then, the analysis addresses the symmetric arrangement more in detail, in order to capture helpful guidelines about the possible interchangeability between the viscous and dry models of the internal friction. Quite similar stability conditions are found for balanced rotors subject to viscous or dry dissipation. While the linear case may be faced by the Routh Hurwitz procedure, the non-linear one may be dealt with by numerical procedures, but the actual situation is better elucidated by perturbation approaches, e. g. of the Krylov-Bogoliubov type, which may give a valid quantitative indication on the stability thresholds throughout the whole speed range.

MATHEMATICAL MODEL

Figure 1 shows the rotor-suspension system and may be used as a reference for the notation. The approach is similar to ref. [2-5, 22]. The rotor is subject to a static unbalance, specified by the location of the mass centre C at some fixed eccentricity e from the intersection O_1 of the shaft axis with the rotor diametral plane, and to a

dynamic unbalance, which may be schematized by two equal fictitious point masses m_d , symmetric with respect to O_1 , lying on a meridian plane which does not contain C in general. The masses of the support are neglected. The torsional deformation between the rotor and the end sections is ignored, as the torsional motion is uncoupled with the bending motion within the linear approximation.

The frame $Cxyz$ moves with C remaining parallel to the fixed frame $Ox_0y_0z_0$, while the frame $C\xi\eta\zeta$ is obtainable by another auxiliary frame fixed to the rotor, through a backward rotation of the diametral axes ξ and η around ζ of an angle equal to the rotor rotation $\theta = \omega t$. Then, the reference $C\xi\eta\zeta$ does not partake in the main rotating motion with angular speed ω , but performs only the small rotations φ and ψ around the axes x and y due to the shaft deflection. Furthermore, the shaft is supposed horizontal and the gravitational field g is assumed directed towards $-y_0$.

The differentiation with respect to the dimensionless angular time variable $\theta = \omega t$ is indicated with primes, whence $d(\dots)/dt = \omega(\dots)'$, etc. Moreover, defining a reference shaft stiffness k_0 , taken for example from the fixed support case ($k_0 = 48EI/l_s^3$ for two self-aligning bearings, or $k_0 = 192EI/l_s^3$ for two cylindrical bearings, where EI is the flexural stiffness and l_s the shaft length) and defining a reference critical speed $\omega_c = \sqrt{k_0/m}$, the angular speed ratio $\Omega = \omega/\omega_c$ may be introduced, together with the dimensionless stiffness ratios, $K_{3x} = k_{3x}/k_0$, $K_{3y} = k_{3y}/k_0$, $K_{4x} = k_{4x}/k_0$ and $K_{4y} = k_{4y}/k_0$, assuming different support stiffness in the horizontal and vertical planes. As regards the self-weight effects, the dimensionless gravity parameter $\Gamma = mg/(ek_0)$ is introduced.

Some external environmental dissipation is supposed to act on the rotor translational and rotational motions and the correspondent resistances are assumed viscous-like and linear for simplicity, whence the viscous equivalent coefficients c_1 [$\text{kg}\cdot\text{s}^{-1}$] and c_2 [$\text{kg}\cdot\text{m}^2\cdot\text{s}^{-1}$] are introduced, together with the damping factors $d_1 = 0.5c_1\omega_c/k_0$ and $d_2 = 0.5c_2\omega_c/(k_0l_s^2)$. Similarly, the damping factors $d_{3x} = 0.5c_{3x}\omega_c/k_0$, $d_{3y} = 0.5c_{3y}\omega_c/k_0$, $d_{4x} = 0.5c_{4x}\omega_c/k_0$, $d_{4y} = 0.5c_{4y}\omega_c/k_0$, are ascribed to the horizontal and vertical damping of the suspension system, where the c 's stand for viscous damping coefficients of the supports.

Similarly to [2-5], the shaft is considered massless, elastic and hysteretic, and the internal dissipative force acting on the rotor is assumed opposite to the velocity $\mathbf{v}_{\text{rel.}}$ of point O_1 relative to a reference system $O_3\xi_0\eta_0\zeta_0$ having the coordinate axis ζ_0 through the centres of the shaft end sections and rotating with the driving end section at the same angular speed ω (see detail of Fig. 1). Indicating with $L_3 = -z_3/l_s$ and $L_4 = z_4/l_s$ the dimensionless distances of the rotor from the shaft ends, the components of $\mathbf{v}_{\text{rel.}}$ in the fixed reference $Ox_0y_0z_0$ are $v_{\text{rel.,}x} = \dot{x}_1 - \dot{x}_3L_4 - \dot{x}_4L_3 + \omega(y_1 - y_3L_4 - y_4L_3)$ and $v_{\text{rel.,}y} = \dot{y}_1 - \dot{y}_3L_4 - \dot{y}_4L_3 - \omega(x_1 - x_3L_4 - x_4L_3)$. For viscous-like internal friction, the hysteresis force on the rotor is given by the product of the relative velocity and a hysteretic coefficient c_h : $\mathbf{F}_h = -c_h\mathbf{v}_{\text{rel.}}$. The correspondent forces on the two supports are given by $\mathbf{F}_{3h} = -L_4\mathbf{F}_h$, $\mathbf{F}_{4h} = -L_3\mathbf{F}_h$. In the hypothesis of Coulomb friction, a different model must be applied: $\mathbf{F}_h = -F_{h,\text{dry}}\mathbf{v}_{\text{rel.}}/|\mathbf{v}_{\text{rel.}}|$, where the coefficient $F_{h,\text{dry}}$ is the friction force level.

Considering the steady rotation of a perfectly balanced weighty rotor immersed horizontally in the gravity field, the shaft deflection plane is motionless and counter-rotates with opposite angular speed with respect to the reference frame $O_3\xi_0\eta_0\zeta_0$ fixed to the shaft end sections. Therefore, point O_1 travels along a circular path in this reference frame and the hysteretic work done during one single revolution is given by the integral $c_h \oint (v_{rel.,x}^2 + v_{rel.,y}^2) dt = c_h \omega \oint [(y_1 - L_4 y_3 - L_3 y_4)^2 + (-x_1 + L_4 x_3 + L_3 x_4)^2] d\theta$, where x_j and y_j are equilibrium values. Assuming that this work is proportional to the square of the path radius and independent of ω , it is easy verifiable that the product $c_h \omega$ must be considered constant on varying ω , whence a constant hysteresis factor $d_h = 0.5 c_h \omega / k_0$ may be introduced (see [23]).

The presence of some unbalance induces a further rotating bending of the shaft around the equilibrium configuration, with the same angular speed ω , and, in case of isotropic stiffness and damping of the supports, i. e. for $K_{3x} = K_{3y}$, $K_{4x} = K_{4y}$, $d_{3x} = d_{3y}$, $d_{4x} = d_{4y}$, this motion is circularly polarized, does not imply any relative velocity with respect to the frame $O_3\xi_0\eta_0\zeta_0$ and is uninfluential on the overall friction work. In the case of suspension anisotropy on the contrary, the unbalanced trajectories are elliptical and thus, transforming the coordinates from the fixed frame to the rotating frame $O_3\xi_0\eta_0\zeta_0$, the paths take double looped shapes and are covered by twice the shaft frequency, i. e. with the angular speed 2ω , because the radius vector is subject to increasing and decreasing phases twice during one full revolution of the rotating frame.

Following [23], the two mentioned dissipative cycles must be dealt with separately and two different hysteresis coefficients c_h must be defined, the one, c_{h1} , for the frequency ω and the other, c_{h2} , for the double frequency 2ω . As it is reasonable to assume that $\omega c_{h1} = 2\omega c_{h2} = h$ [23], where h is a hysteresis constant of the material, two hysteresis factors must be introduced, $d_{h1} = 0.5 h / k_0$ for the relative rotation of the equilibrium deflection plane and $d_{h2} = 0.25 h / k_0 = d_{h1} / 2$ for the elliptical motions due to the unbalance. The hysteresis factor d_{h1} will be used for the equilibrium configuration, while d_{h2} will be used for the frequency response to the unbalance. When applying the small perturbation procedure to check the system stability, very small deviations of the perturbed trajectories from the steady paths will be assumed and the factor d_{hi} will be kept unmodified. The use of the first or the second hysteresis factor in the stability analysis will depend on the prevalence of the gravity or the unbalance effect on the rotor response, $\Gamma = mg/(ek_0) > 1$ or $\Gamma = mg/(ek_0) < 1$.

If the internal dissipation is of the dry friction type, the work per cycle is $F_{h,dry} \oint \sqrt{v_{rel.,x}^2 + v_{rel.,y}^2} dt$ and a dry damping factor must be defined: $d_{h,dry} = F_{h,dry} / (k_0 e)$. The equivalence between dry and viscous friction can be stated and checked on the basis of the same energy dissipation during a sufficiently large number of revolutions and the parameters $d_{h,dry}$ and d_h can be thus correlated with each other.

Introduce the dimensionless displacement-rotation vectors $\mathbf{X} = \{X_1, X_2, X_3, X_4\}^T$ and $\mathbf{Y} = \{Y_1, Y_2, Y_3, Y_4\}^T$, where, using the subscripts 1, 3, 4 for the displacements of the rotor and the support and 2 for the rotor tilt around y and x , it was put $X_j = x_j/e$, $Y_j = y_j/e$, for $j \neq 2$, and $X_2 = \psi/e$, $Y_2 = -\phi/e$ (the minus sign in the definition of Y_2 permits using the same stiffness matrix for both the bending planes, xz and yz).

Scaling all forces and moments by k_0e and k_0e/l respectively, considering self-aligning bearings, introducing the dimensionless stiffness matrices K_{jz} in the inflexion planes xz ($j = x$) and yz ($j = y$),

$$\mathbf{K}_{jz} = \frac{1}{16L_3^3L_4^3} \begin{bmatrix} 1-3L_3L_4 & L_3L_4(L_3-L_4)/c & -L_4^3 & -L_3^3 \\ L_3L_4(L_3-L_4)/c & L_3^2L_4^2/(2c-1) & L_3L_4^3/c & -L_4L_3^3/c \\ -L_4^3 & L_3L_4^3/c & 16L_3^3L_4^3K_{3j}+L_4^3 & 0 \\ -L_3^3 & -L_4L_3^3/c & 0 & 16L_3^3L_4^3K_{4j}+L_3^3 \end{bmatrix} \quad (1)$$

where $c = 1$ or 2 for hinged-hinged or clamped-clamped shafts ($c = 1$ in the following), and the hysteretic matrices \mathbf{H}_i for $i = 1$ or 2 (frequency ω or 2ω)

$$\mathbf{H}_i = d_{hi} \begin{bmatrix} 1 & 0 & -L_4 & -L_3 \\ 0 & 0 & 0 & 0 \\ -L_4 & 0 & L_4^2 & L_3L_4 \\ -L_3 & 0 & L_3L_4 & L_3^2 \end{bmatrix} \quad (2)$$

the equations of motion can be written in the form

$$\mathbf{K}_{xz}\mathbf{X} + 2\Omega\mathbf{D}_{xz}\mathbf{X}' + 2\mathbf{H}_i(\mathbf{X}' + \mathbf{Y}) + \Omega^2\mathbf{M}\mathbf{X}'' + \Omega^2\mathbf{G}\mathbf{Y}' - \begin{Bmatrix} \Omega^2 \cos \theta \\ -M_d\Omega^2 \cos(\theta - \gamma) \\ 0 \\ 0 \end{Bmatrix} = 0 \quad (3a,b)$$

$$\mathbf{K}_{yz}\mathbf{Y} + 2\Omega\mathbf{D}_{yz}\mathbf{Y}' + 2\mathbf{H}_i(\mathbf{Y}' - \mathbf{X}) + \Omega^2\mathbf{M}\mathbf{Y}'' - \Omega^2\mathbf{G}\mathbf{X}' - \begin{Bmatrix} \Omega^2 \sin \theta - \Gamma \\ -M_d\Omega^2 \sin(\theta - \gamma) \\ 0 \\ 0 \end{Bmatrix} = 0$$

where $M_d = 0.5 m_d s_r d_r / e l_s m$ is a dynamic unbalance number, s_r and d_r being the axial size and the diameter of the rotor (see Fig. 1), and γ is the angle between the meridian planes through C and through the point masses m_d . Moreover, $J_d = j_d / m l_s^2$ and $J_a = j_a / m l_s^2$ are the dimensionless diametral and axial moment of inertia of the rotor, scaled by the product $m l_s^2$, j_d and j_a being the real moment of inertia, evaluated in the absence of dynamic unbalance, and the matrices \mathbf{D}_{jz} ($j = x, y$), \mathbf{M} and \mathbf{G} are diagonal and are the viscous, massive and gyroscopic matrices, whose coefficients are $(d_1, d_2, d_{3j}, d_{4j})$, $(1, J_d, 0, 0)$ and $(0, J_a, 0, 0)$ respectively.

RESULTS FOR THE GENERAL ASYMMETRIC CASE

The equilibrium configuration is obtainable rewriting Eqs. (3) in the form $\mathbf{K}_{xz}\mathbf{X}_{eq.} + 2\mathbf{H}_1\mathbf{Y}_{eq.} = 0$, $\mathbf{K}_{yz}\mathbf{Y}_{eq.} - 2\mathbf{H}_1\mathbf{X}_{eq.} = -\Gamma \{1, 0, 0, 0\}^T$. This algebraic system leads to the

solution, $\mathbf{X}_{eq.} = 2\Gamma\mathbf{A}_{xz}\mathbf{H}_1(\mathbf{K}_{yz} + 4\mathbf{H}_1\mathbf{A}_{xz}\mathbf{H}_1)^{-1}\{1, 0, 0, 0\}^T$, $\mathbf{Y}_{eq.} = -\Gamma(\mathbf{K}_{yz} + 4\mathbf{H}_1\mathbf{A}_{xz}\mathbf{H}_1)^{-1}\{1, 0, 0, 0\}^T$, where $\mathbf{A}_{jz} = \mathbf{K}_{jz}^{-1}$ are the flexibility matrices, and introducing the 2×2 shaft flexibility sub-matrix $[\mathbf{A}_0]$ (fixed supports)

$$\mathbf{A}_0 = 16 \begin{bmatrix} L_3^2 L_4^2 & L_3 L_4 (L_4 - L_3) \\ L_3 L_4 (L_4 - L_3) & 1 - 3L_3 L_4 \end{bmatrix}$$

this solution can be written in the form

$$\mathbf{X}_{eq.} = \frac{2d_{h1}\Gamma\mathbf{A}_{0,11}}{1 + 4d_{h1}^2\mathbf{A}_{0,11}^2} \begin{bmatrix} \mathbf{A}_{0,11} \\ \mathbf{A}_{0,21} \\ 0 \\ 0 \end{bmatrix} \quad \mathbf{Y}_{eq.} = -\Gamma \begin{bmatrix} \frac{\mathbf{A}_{0,11}}{1 + 4d_{h1}^2\mathbf{A}_{0,11}^2} + \frac{L_3^2}{K_{4y}} + \frac{L_4^2}{K_{3y}} \\ \frac{\mathbf{A}_{0,21}}{1 + 4d_{h1}^2\mathbf{A}_{0,11}^2} - \frac{L_4}{K_{3y}} + \frac{L_3}{K_{4y}} \\ \frac{L_4}{K_{3y}} \\ \frac{L_3}{K_{4y}} \end{bmatrix} \quad (4a,b)$$

As $X_{1eq.}$ and $X_{2eq.}$ are positive for $d_{h1} \neq 0$, while $X_{3eq.} = X_{4eq.} = 0$, the hysteresis appears to produce a constant bias of the inflexion plane, concordant with the angular speed, while the static support deflection occurs in the vertical plane. Equations (4) show also that the static rotor displacement is small of order d_{h1} in the horizontal direction, whereas the changes of the vertical displacement due to hysteresis are of order d_{h1}^2 .

The natural precession modes of the rotor-shaft system are obtainable ignoring the forcing and dissipative terms in Eqs. (3). Defining with \mathbf{K}_{ij}^{kl} the 2×2 matrix extracted by a generic 4×4 matrix \mathbf{K} considering only the elements of rows i and j and columns k and l , putting $\bar{\mathbf{K}}_x = \mathbf{K}_{12}^{12} - \mathbf{K}_{12}^{34}(\mathbf{K}_{34}^{34})^{-1}\mathbf{K}_{34}^{12}$, $\bar{\mathbf{K}}_y = \mathbf{K}_{12}^{12} - \mathbf{K}_{12}^{34}(\mathbf{K}_{34}^{34})^{-1}\mathbf{K}_{34}^{12}$, $X_j = X_{j0} \exp(i\Omega_n\theta/\Omega)$, $Y_j = -iY_{j0} \exp(i\Omega_n\theta/\Omega)$, where the dimensionless precession speed $\Omega_n = \omega_n / \omega_c$ was introduced, the characteristic equation is a fourth degree algebraic equation in Ω_n^2 , dependent on Ω^2

$$\begin{aligned} & [(\bar{K}_{x11} - \Omega_n^2)(\bar{K}_{x22} - J_d\Omega_n^2) - \bar{K}_{x12}^2][(\bar{K}_{y11} - \Omega_n^2)(\bar{K}_{y22} - J_d\Omega_n^2) - \bar{K}_{y12}^2] = \\ & = (\bar{K}_{x11} - \Omega_n^2)(\bar{K}_{y11} - \Omega_n^2)J_a^2\Omega^2\Omega_n^2 \end{aligned} \quad (5)$$

The choice between the plus or minus sign for $\Omega_n = \pm\sqrt{\Omega_n^2}$ after solving Eq. (5) for Ω_n^2 , may be done in view of getting equal signs for the amplitudes $X_{1,0}$ and $Y_{1,0}$, whence the whirling motion of the rotor centre is a progressive or retrograde precession for $\Omega_n > 0$ or $\Omega_n < 0$.

Figures 2 show the Campbell diagrams for two examples cases, of an oblong and an oblate ellipsoid of inertia of the rotor. The left diagrams refer to isotropic support

stiffness and the right ones to anisotropic stiffness. The continuous lines represent forward/backward whirl and refer to the motion of point O_1 , together with the other motions with the same whirl direction. When on the contrary the whirl direction of one support or of the rotor axis is counter-directed with respect to the rotor centre, a plot with small circles or crosses is reported, symmetric of course of another continuous branch. Only equal-directed whirling motions may develop for isotropic support stiffness, whereas some whirling directions may be opposite to the rotor centre, when the supports have quite different stiffness values on the two planes.

The response to unbalance can be detected replacing $\mathbf{X} = \mathbf{X}_{c0} \cos \theta + \mathbf{X}_{s0} \sin \theta$, $\mathbf{Y} = \mathbf{Y}_{c0} \cos \theta + \mathbf{Y}_{s0} \sin \theta$ into Eqs. (3) and applying a harmonic balance procedure. A 16×16 algebraic system is obtained, whose solutions permits calculating the steady elliptical paths of the rotor and the supports.

The principal half-diameters and their angles with the fixed reference frame are:

$$a_j = \sqrt{\frac{Y_{c0,j}^2 + Y_{s0,j}^2 + X_{c0,j}^2 + X_{s0,j}^2 \pm \sqrt{(Y_{c0,j}^2 + Y_{s0,j}^2 - X_{c0,j}^2 - X_{s0,j}^2)^2 + 4(X_{c0,j}Y_{c0,j} + X_{s0,j}Y_{s0,j})^2}}{2}}$$

$$b_j = \sqrt{\frac{Y_{c0,j}^2 + Y_{s0,j}^2 + X_{c0,j}^2 + X_{s0,j}^2 \mp \sqrt{(Y_{c0,j}^2 + Y_{s0,j}^2 - X_{c0,j}^2 - X_{s0,j}^2)^2 + 4(X_{c0,j}Y_{c0,j} + X_{s0,j}Y_{s0,j})^2}}{2}}$$

(6a,b)

$$\tan 2\phi_j = \frac{2(X_{c0,j}Y_{c0,j} + X_{s0,j}Y_{s0,j})}{X_{c0,j}^2 + X_{s0,j}^2 - Y_{c0,j}^2 - Y_{s0,j}^2}$$

As an example, Figure 3a shows the equilibrium points and the steady elliptical trajectories of the rotor and the supports during a complete wobbling cycle, for a particular under-critical case. Figure 3b shows the path of point O_1 in the rotating reference $O_3\xi_0\eta_0\zeta_0$, pointing out the double looped shape of the trajectory during one complete revolution.

The frequency response for the four whirling motions is also reported in Figs. 4 as an example. The figures show the major and minor radii of the elliptical paths and the angle ϕ of the major axis with respect to the horizontal plane. It is observable that the rotor trajectory tends to a circle with radius equal to the mass eccentricity e for $\Omega \rightarrow \infty$, similarly to the conventional Laval-Jeffcott behaviour: the centre of mass tends to its centred motionless position.

Stability of the Steady Motion

The motion stability can be inspected throughout the speed range by some perturbation approach, putting $\mathbf{X} = \mathbf{X}_{\text{steady}} + \tilde{\mathbf{X}}$, $\mathbf{Y} = \mathbf{Y}_{\text{steady}} + \tilde{\mathbf{Y}}$, where the subscript \dots_{steady} indicates the previous steady solutions and the tilde refers to the small perturbations.

Assuming solutions of the type $\tilde{\mathbf{X}} = \tilde{\mathbf{X}}_0 \exp(\sigma\theta / \Omega)$, $\tilde{\mathbf{Y}} = \tilde{\mathbf{Y}}_0 \exp(\sigma\theta / \Omega)$, where σ is a characteristic number, using the previous notation and the hysteretic factors d_{h1} or d_{h1} in accordance with the prevailing of the gravity or the unbalance influence in the system under examination, one gets a twelfth degree characteristic equation, $E_c(\sigma) = b_0\sigma^{12} + b_1\sigma^{11} + \dots + b_j\sigma^{12-j} + \dots + b_{11}\sigma + b_{12} = 0$, where the coefficient b_0 of σ^{12} is equal to $16J_d^2[d_{3x}d_{4x} + d_{hi}(d_{3x}L_3^2 + d_{4x}L_4^2)/\Omega] [d_{3y}d_{4y} + d_{hi}(d_{3y}L_3^2 + d_{4y}L_4^2)/\Omega] > 0$. As

regards the other coefficients, a collocation method may be applied, choosing six values σ_i arbitrarily for $i = 1, 2, \dots, 6$, evaluating $E_c(\sigma_i)$ and $E_c(-\sigma_i)$ and composing two uncoupled 6×6 algebraic systems for the even and odd coefficients b_j :

$$\frac{E_c(\sigma_i) + E_c(-\sigma_i)}{2} - b_0 \sigma_i^{12} = b_2 \sigma_i^{10} + b_4 \sigma_i^8 + b_6 \sigma_i^6 + b_8 \sigma_i^4 + b_{10} \sigma_i^2 + b_{12} \quad (\text{for } i = 1 \text{ to } 6) \quad (7)$$

$$\frac{E_c(\sigma_i) - E_c(-\sigma_i)}{2} = b_1 \sigma_i^{11} + b_3 \sigma_i^9 + b_5 \sigma_i^7 + b_7 \sigma_i^5 + b_9 \sigma_i^3 + b_{11} \sigma_i$$

Then, the usual Routh-Hurwitz procedure can be applied to calculate the thresholds of stability, i. e. the levels of the external viscous damping needed to nullify the destabilizing effect of the internal hysteresis. This is done exploring the speed range carefully for several values of the geometrical and mechanical parameters of the rotor-shaft-support system and increasing the external viscous damping stepwise by a trial and error technique. The main features of the system behaviour are reported in the examples of Fig. 5, where the damping factors d_1 and d_2 were chosen null and all the others were assumed equal ($d_{3x} = d_{3y} = d_{4x} = d_{4y} = d_s$).

Figure 5a reports the stability threshold d_s in dependence on the geometrical location of the rotor along the shaft. In particular, it shows the effect of the stiffness anisotropy of the supports. It is interesting that the increase in the stiffness anisotropy improves the stability of the whirling motion mainly if the rotor is mounted at the mid-span of the shaft. Actually, no external viscous dissipation source is required for symmetric systems if the relative difference between horizontal and vertical stiffness is larger than a certain limit value. This result agrees with the ones of the following section and with reference [9], but it is here clearly shown how the beneficial influence of the support anisotropy decreases on shifting the rotor towards the one or the other support, unless the suspension system is isotropic, in which case the worst stability conditions are just found in the symmetric configuration. Observe that, on increasing the difference $K_y - K_x$, the curves of Fig. 5a begin to show a sort of dip near $L_3 \cong 0.4$, which becomes more and more pronounced until turning the curve towards the point $L_3 = 0.5$, $d_s = 0$ for higher stiffness gaps (perfect stabilization). In this region however, the diagrams are quite steep, so that the best benefit of the suspension anisotropy appears confined in a rather narrow interval astraddle the mid-span, though it remains always favourable with respect to the pure isotropic case $K_y = K_x$ also for moderate values of $K_y - K_x$. Thus, the results of previous studies (e. g. [9]) are confirmed but appear strongly limited by an even small change of the rotor position in the neighbourhood of the shaft middle section.

Figure 5b shows similar plots, but focuses on the gyro structure, which is found to exert a slight but clear destabilizing effect and in fact, the case of a spherical ellipsoid of inertia of the rotor ($J_a = J_d$) requires the lowest additional viscous damping to stabilize the rotor whirl.

The influence of the elastic dissymmetry between the front and back suspension is shown in Fig. 5c, whose diagrams may be prolonged for $L_3 > 0.5$ by mirror interchange of the two lower curves. These plots indicate the convenience of a more flexible suspension of the support closest to the rotor, particularly if the rotor is

mounted roughly halfway between the mid-span and the support. On the other hand, it is to be observed that all diagrams of Figs. 5 a,b,c,d indicate in general a stabilizing effect of the geometrical asymmetry of the rotor configuration and a negligible influence of the shaft hysteresis for $L_3 \rightarrow 0$.

At last, the case of "infinite" vertical stiffness (journal boxes moving only horizontally) is compared in Fig. 5d with the isotropic stiffness case: the unidirectional support compliance appears here much more convenient with respect to the axial-isotropic case.

The stability control can be also carried out by numerical integration, starting from random initial values and using some proper routine, for example of the Euler-Cauchy or Runge-Kutta types, though this kind of approach is more wearisome. Nevertheless, this turns out to be a convenient procedure when modelling the internal dissipation by dry friction. Assuming such a friction model as the most appropriate for a particular system, the internal hysteretic force acting on the rotor has to be considered constant and opposite to the relative velocity with respect to the rotating frame shown in the detail of Fig. 1, and has thus the two components $F_{hx} = -F_{h,dry} v_{rel.,x} / \sqrt{v_{rel.,x}^2 + v_{rel.,y}^2}$, $F_{hy} = -F_{h,dry} v_{rel.,y} / \sqrt{v_{rel.,x}^2 + v_{rel.,y}^2}$. Furthermore, it is to be observed that the differential system (3a,b) is of the twelfth order, due to the neglect of the support masses, and when integrating numerically, the third and fourth equations of (3a) and (3b) must be solved in advance for the four derivatives, X'_3 , X'_4 , Y'_3 , Y'_4 at each step. This task can be fulfilled by simple inversion of sub-matrices in the viscous linear case, but must be carried out by some iterative procedure in the dry non-linear one.

The numerical integration of Eqs. (3) permits comparing the results obtainable by the viscous and dry models. To this end, some equivalence criterion must be stated between the coefficients $F_{h,dry}$ and c_h or else between the hysteresis factors $d_{h,dry} = F_{h,dry}/k_0 e$ and $d_h = 0.5c_h \omega/k_0$, and this may be done for example by imposing the same dissipated work over a period of several revolutions of the rotor: $d_{h,dry} = 2d_h \int_{\theta}^{\theta+2N\pi} (\xi_0'^2 + \eta_0'^2) d\theta / \int_{\theta}^{\theta+2N\pi} e \sqrt{\xi_0'^2 + \eta_0'^2} d\theta$ where $N \gg 1$. During the calculation of the diagrams reported in the following figures 6, the dry coefficient $d_{h,dry}$ was updated at the end of each long period according to this equivalence criterion, until it reached a nearly invariable asymptotic value. Then, the numerical integration re-started using this asymptotic value.

Figure 6a shows the transient path of point O_1 , in the viscous and dry assumption, for a stable under-critical case. As clearly observable, the two diagrams exhibit nearly the same evolution and tend to the same elliptical path. On the contrary, Figure 6b refers to an unstable over-critical case, but shows that the two trajectories are roughly similar. Moreover, checking several working conditions close to the stability threshold, it is observable that the threshold is reached for slightly higher levels of the external damping by the linear hysteretic model than by the Coulombian one. As a result, it appears that the viscous hysteretic hypothesis can be conveniently applied also in the case of uncertainty about the amount of Coulombian friction within the whole internal dissipation, giving quite conservative results.

ANALYTICAL APPROACHES TO THE SYMMETRIC CASE

The effect of the stiffness anisotropy may be better elucidated by analysing a rotor mounted at the mid-span of a shaft on symmetric supports, $K_{3x} = K_{4x} = K_{x,tot.}/2$, $K_{3y} = K_{4y} = K_{y,tot.}/2$, with equal damping factors, $d_{3x} = d_{4x} = d_{3y} = d_{4y} = d_{s,tot.}/2$, and zero external dissipative forces on the rotor, $d_1 = d_2 = 0$. In this case, the conical whirl is uncoupled with the cylindrical whirl and is independent of the hysteresis and stable. Actually, all the following approaches for the simpler symmetric case could also be extended and adapted to the general asymmetric case, but would just replace its original differential system with another one to be solved numerically all the same and would not yield straightforward analytical results.

Putting $X_1 = X_r$, $X_3 + X_4 = 2X_s$, $Y_1 = Y_r$, $Y_3 + Y_4 = 2Y_s$, observing that $K_{jz11} = -2K_{jz13} = -2K_{jz14} = 1$, $2K_{jz33} = 2K_{jz44} = 1 + K_{j,tot.}$ (for $j = x$ or y), the perturbed cylindrical motions included in Eqs. (3a) and (3b) may be described by the simpler differential system:

$$\begin{aligned}
 X_r - X_s + 2d_{hi}(X_r' - X_s' + Y_r - Y_s) + \Omega^2 X_r'' &= 0 \\
 -X_r + (1 + K_{x,tot.})X_s + 2\Omega d_{s,tot.}X_s' - 2d_{hi}(X_r' - X_s' + Y_r - Y_s) &= 0 \\
 Y_r - Y_s + 2d_{hi}(Y_r' - Y_s' - X_r + X_s) + \Omega^2 Y_r'' &= 0 \\
 -Y_r + (1 + K_{y,tot.})Y_s + 2\Omega d_{s,tot.}Y_s' - 2d_{hi}(Y_r' - Y_s' - X_r + X_s) &= 0
 \end{aligned} \tag{8a,b,c,d}$$

where the tildes have been omitted.

Replacing solutions of the type $\exp(\sigma\theta/\Omega)$, it is easy to arrive at the sixth degree characteristic equation

$$(H^2 + 4d_{hi}^2)(A_x + \sigma^2)(A_y + \sigma^2) + \sigma^4 A_x A_y + \sigma^2 H[A_x(A_y + \sigma^2) + A_y(A_x + \sigma^2)] = 0 \tag{9}$$

where $H = 1 + 2d_{hi}\sigma/\Omega$, $A_x = K_{x,tot.} + 2d_{s,tot.}\sigma$, $A_y = K_{y,tot.} + 2d_{s,tot.}\sigma$, and it is observable that the fifth Routh-Hurwitz determinant RH_5 is the first one that becomes critical on increasing the hysteresis factor d_{hi} . Neglecting the viscous damping, in order to assess the self-stabilizing aptitude of the system, and assuming the realistic hypothesis that $(2d_{hi}/\Omega)^2 \ll 1$, this determinant may be ascertained as positive and then stable if the difference $(K_{y,tot.} - K_{x,tot.})$ is of the same order of magnitude of $K_{x,tot.}$ and $K_{y,tot.}$. When on the contrary $(K_{y,tot.} - K_{x,tot.})$ is of order d_{hi} , one can find that the dominant part of RH_5 is given by $RH_5 \cong (2 + K_{x,tot.} + K_{y,tot.})(K_{x,tot.}K_{y,tot.})^2(2d_{hi}/\Omega)^3\{(K_{y,tot.} - K_{x,tot.})^2 - 8d_{hi}^2[(K_{y,tot.} - K_{x,tot.})^2 + 2(K_{x,tot.}K_{y,tot.})^2]\}$, whence the following stability limit may be obtained irrespective of the angular speed

$$\left| \frac{K_{x,tot.}K_{y,tot.}}{K_{y,tot.} - K_{x,tot.}} \right| < \sqrt{\frac{1}{16d_{hi}^2} - \frac{1}{2}} \cong \frac{1}{4d_{hi}} \tag{10}$$

This result is in perfect accordance with Fig. 5 a,b for $L_3 = 1/2$ and points out how the elastic anisotropy of the supports may exert a strong stabilizing effect.

Small Perturbation Procedure

Putting $\mathbf{U} = \mathbf{X} + i\mathbf{Y}$, $\mathbf{V} = \mathbf{X} - i\mathbf{Y}$, multiplying Eqs. (8c) and (8d) by the imaginary unit i , summing and subtracting them from Eqs. (8a) and (8b) respectively, one gets

$$\begin{aligned}
 U_r - U_s + 2d_{hi}[(U_r' - U_s') - i(U_r - U_s)] + \Omega^2 U_r'' &= 0 \\
 -U_r + \left(1 + \frac{K_{x,tot.} + K_{y,tot.}}{2}\right)U_s + \frac{K_{x,tot.} - K_{y,tot.}}{2}V_s + 2\Omega d_{s,tot.}U_s' + \\
 -2d_{hi}[(U_r' - U_s') - i(U_r - U_s)] &= 0
 \end{aligned} \tag{11a,b,c,d}$$

$$\begin{aligned}
 V_r - V_s + 2d_{hi}[(V_r' - V_s') + i(V_r - V_s)] + \Omega^2 V_r'' &= 0 \\
 -V_r + \left(1 + \frac{K_{x,tot.} + K_{y,tot.}}{2}\right)V_s + \frac{K_{x,tot.} - K_{y,tot.}}{2}U_s + 2\Omega d_{s,tot.}V_s' + \\
 -2d_{hi}[(V_r' + V_s') + i(V_r - V_s)] &= 0
 \end{aligned}$$

In the hypothesis that the dissipative factors d_s and d_{hi} are small, the characteristics roots of system (11) are very close to the natural frequencies Ω_n . Therefore, putting $\mathbf{U} = \mathbf{U}_0 \exp(i\sigma\theta/\Omega)$, $\mathbf{V} = \mathbf{V}_0 \exp(i\sigma\theta/\Omega)$, where σ is nearly real and very close to one of the Ω_n 's and the constant vectors \mathbf{U}_0 and \mathbf{V}_0 are nearly real as well, it is easy to recognize that \mathbf{U} and \mathbf{V} describe progressive and retrograde precession motions respectively for $\text{Real}(\sigma) > 0$, or vice versa for $\text{Real}(\sigma) < 0$, which motions are coupled with each other through the differential stiffness coefficient $(K_{x,tot.} - K_{y,tot.})/2$. In accordance with the elliptic shape of the orbital paths, all natural modes turn out to be composed of progressive and retrograde circular motions, which become uncoupled for $K_{x,tot.} = K_{y,tot.}$. Notice that the ideal non-dissipative natural modes are uncoupled in the horizontal and vertical planes by Eqs. (8a,b,c,d).

All small parameters can be scaled by d_{hi} , putting $d_{s,tot.} = \delta d_{hi}$ and $\sigma = \Omega_n + i\lambda d_{hi}$, where δ and λ are numbers of order one and stability requires the real part of λ to be positive, in order that the real part of $i\sigma$ is negative. Replacing the above exponential solutions into Eqs. (11a,b,c,d) and retaining only the terms of order 1 and d_{hi} , one gets a complex algebraic system for U_{r0} , U_{s0} , V_{r0} , V_{s0} , whose coefficients are given by the matrix

$$\begin{bmatrix}
 1 - \Omega_n^2 + 2id_{hi}(s^{(-)} - \lambda\Omega_n) & -1 - 2id_{hi}s^{(-)} & 0 & 0 \\
 -1 - 2id_{hi}s^{(-)} & 1 + \frac{K_{x,tot.} + K_{y,tot.}}{2} + 2id_{hi}(s^{(-)} + \delta\Omega_n) & 0 & \frac{K_{x,tot.} - K_{y,tot.}}{2} \\
 0 & 0 & 1 - \Omega_n^2 + 2id_{hi}(s^{(+)} - \lambda\Omega_n) & -1 - 2id_{hi}s^{(+)} \\
 0 & \frac{K_{x,tot.} - K_{y,tot.}}{2} & -1 - 2id_{hi}s^{(+)} & 1 + \frac{K_{x,tot.} + K_{y,tot.}}{2} + 2id_{hi}(s^{(+)} + \delta\Omega_n)
 \end{bmatrix} \tag{12}$$

where one has put $s^{(-)} = \Omega_n/\Omega - 1$ and $s^{(+)} = \Omega_n/\Omega + 1$. Cancelling the terms containing $2id_{hi}$, we get the characteristic equation for the natural frequencies:

$$\left[\left(1 + \frac{K_{x,tot.} + K_{y,tot.}}{2} \right) (1 - \Omega_n^2) - 1 \right]^2 - \left(\frac{K_{x,tot.} - K_{y,tot.}}{2} \right)^2 (1 - \Omega_n^2)^2 = 0 \tag{13}$$

whence $\Omega_n^2 = 1/(1 + 1/K_{x,tot. \text{ or } y,tot.})$.

The first order correction λ to the eigenvalues of system (11) may be obtained multiplying the terms with $2id_{hi}$ in the determinant of (12) by their own cofactors in the ideal matrix with $d_{hi} = 0$. After some algebra, one gets

$$2id_{hi} \left[\left(1 + \frac{K_{x,tot.} + K_{y,tot.}}{2} \right) (1 - \Omega_n^2) - 1 \right] \left[\frac{\Omega_n}{1 - \Omega_n^2} \right] \left[(s^{(-)} + s^{(+)}) \Omega_n^3 + 2\delta(1 - \Omega_n^2)^2 - 2\lambda \right] = 0 \quad (14)$$

Since the quantity $(s^{(-)} + s^{(+)}) \Omega_n^3 = 2\Omega_n^4/\Omega$ is always positive, Equations (13) and (14) clearly indicate that λ is real and positive and the motion is stable. Nevertheless, for small anisotropy, i. e. for $(K_{x,tot.} - K_{y,tot.})/2$ of the same order of d_{hi} , the left hand of Eq. (14) becomes of order d_{hi}^2 by Eq. (13) and Equation (14) does no longer hold true in a first approximation analysis, as other terms should be taken into account in the development of the determinant (12): the results from Eq. (14) are then valid only for relatively large anisotropy and reveal stability, in accordance with the previous approach. For $(K_{x,tot.} - K_{y,tot.})/2$ of order d_{hi} on the contrary, one can put $K_m = (K_{x,tot.} + K_{y,tot.})/2$, $\kappa d_{hi} = (K_{x,tot.} - K_{y,tot.})/2$, $K_{x,tot.} = K_m + \kappa d_{hi}$, $K_{y,tot.} = K_m - \kappa d_{hi}$, where $\kappa = O(1)$, and Equation (13) becomes $[(1 + K_m)(1 - \Omega_n^2) - 1]^2 = 0$, whence $\Omega_n^2 = K_m/(1 + K_m)$ twice. The dominant terms of the complete characteristic equation yield

$$\frac{4d_{hi}^2}{(1 + K_m)^2} \left\{ [s^{(-)} K_m^2 + \delta \Omega_n - \lambda \Omega_n (1 + K_m)^2] [s^{(+)} K_m^2 + \delta \Omega_n - \lambda \Omega_n (1 + K_m)^2] + \frac{\kappa^2}{4} \right\} = 0 \quad (15)$$

and, as $s^{(\pm)} = \Omega_n/\Omega \pm 1$ and $\Omega_n = \pm \sqrt{K_m/(1 + K_m)}$, Equation (15) gives

$$\left[\frac{K_m^2}{\Omega} + \delta - \lambda(1 + K_m)^2 \right]^2 \left(\frac{K_m}{1 + K_m} \right) - K_m^4 + \frac{\kappa^2}{4} = 0 \rightarrow \frac{K_m^2}{\Omega} + \delta - \lambda(1 + K_m)^2 = \pm \sqrt{\left(1 + \frac{1}{K_m} \right) \left(K_m^4 - \frac{\kappa^2}{4} \right)} \quad (16)$$

Equation (16) points out that the absolute stability (i. e. for $0 < \Omega < \infty$) can be obtained only for $\delta^2 > (1 + 1/K_m)(K_m^4 - \kappa^2/4)$ if $K_m^4 > \kappa^2/4$, because λ turns out to be always real and positive. The stability is always ensured for any viscous level δ on the contrary, even for $\delta \rightarrow 0$, if $K_m^4 < \kappa^2/4$, which condition confers an imaginary value to λ and is exactly equivalent to Eq. (10), if one minds that $K_{x,tot.} K_{y,tot.} = K_m^2 + O(d_{hi})$ and $\kappa^2/4 = [(K_{x,tot.} - K_{y,tot.})/(4d_{hi})]^2$.

As the perturbed motions under examination are very close to the natural precession motions, it is also possible to opt for a slightly greater precision in the definition of the hysteretic effect and consider such motions affected by their own hysteretic coefficients $c_{hn} = h / |\omega_n - \omega|$, inversely proportional to the relative angular speed $|\omega_n - \omega|$ [23]. Therefore, recalling that $c_{h1} = h / \omega$ and $d_{h1} = 0.5 h / k_0$ for the relative rotation of the equilibrium deflection plane, the hysteretic damping factors d_{hi} of Eq. (11) could be replaced by the more specific ones $d_{hn} = c_{hn} \omega / 2k_0 = (c_{hn}/c_{h1}) h / 2k_0 = d_{h1} / |\Omega_n/\Omega - 1|$. Applying these corrections, the quantities $s^{(\pm)}$ would now stand for $\text{sgn}(\Omega_n/\Omega \pm 1)$ in Eq. (15), whence $s^{(+)} = 1$ and $s^{(-)} = -1$ in the supercritical regime.

As a consequence, Equation (16) would still be applicable, save the disappearance of the term K_m^2 / Ω , and the final result (10) would then remain unchanged.

Should we consider the true isotropic case $K_{x,tot.} = K_{y,tot.} = K_m$, $\kappa = 0$, Equations (11 a,b) would be uncoupled from Eqs. (11 c,d), the ideal natural frequencies would be given by $\Omega_n^2 = K_m / (1 + K_m)$ (twice) and the stability equation (15) would change into $s^{(\pm)} K_m \sqrt{K_m(1+K_m)} + \delta - \lambda (1 + K_m)^2 > 0$, the minus and plus signs referring to progressive and retrograde rotations respectively (**U** progressive and **V** retrograde for $\Omega_n > 0$). While the retrograde motions **V** are stable, the progressive ones **U** may happen to become unstable on increasing the angular speed, as $s^{(-)}$ becomes negative. Nonetheless, the condition of absolute stability ($\lambda > 0$ for $\omega \rightarrow \infty$) would still be $\delta - K_m \sqrt{K_m(1+K_m)} > 0$. It is also remarkable that all the above results are valid for both the hypotheses, that $s^{(\pm)} = \Omega_n / \Omega \pm 1$, or else that $s^{(\pm)} = \text{sgn}(\Omega_n / \Omega \pm 1)$. Summing up, Equation (15) yields the interesting indication that the stabilizing effect of the stiffness anisotropy of the supports is associated in practice to a sort of coupling between progressive and retrograde precession motions ($\kappa > 0$), which coupling is absent in the isotropic systems ($\kappa = 0$).

Autonomous Case: Krylov-Bogoliubov Technique

A new original approach, which may be considered as an extension of the Krylov-Bogoliubov averaging method [24] to several degrees of freedom, can be also applied to the search for the stability threshold of weakly non-linear autonomous systems, i. e. of perfectly balanced rotors. As the calculation is quite laborious, it will be here synthesized, in order to just highlight the main results.

Summing Eqs. (8a) and (8b), summing Eqs. (8c) and (8d), using the damping factor d_{h1} as the rotor is balanced, indicating the small parameter d_{h1} with ε and applying the previous notation for the other quantities, one gets

$$\begin{aligned} \Omega^2 X_r'' + K_m X_s + \varepsilon(2\Omega\delta X'_s + \kappa X_s) &= 0 \\ \Omega^2 X_r'' + X_r - X_s + \varepsilon\Phi_X &= 0 \\ \Omega^2 Y_r'' + K_m Y_s + \varepsilon(2\Omega\delta Y'_s - \kappa Y_s) &= 0 \\ \Omega^2 Y_r'' + Y_r - Y_s + \varepsilon\Phi_Y &= 0 \end{aligned} \tag{17a,b,c,d}$$

and has to put $\Phi_X = (d_{h,dry}/d_{h1})\cos\psi$, $\Phi_Y = (d_{h,dry}/d_{h1})\sin\psi$, $\tan\psi = (Y'_r - Y'_s - X_r + X_s)/(X'_r - X'_s + Y_r - Y_s)$ for non-linear dry friction, whereas putting $\Phi_X = 2(X'_r - X'_s + Y_r - Y_s)$ and $\Phi_Y = 2(Y'_r - Y'_s - X_r + X_s)$ would restore the linear viscous case.

The zero order solution ($\varepsilon = 0$) is $X_r = A\cos(\rho\theta + \alpha)$, $Y_r = B\sin(\rho\theta + \beta)$, $X_s = \Omega_n^2 X_r / K_m$, $Y_s = \Omega_n^2 Y_r / K_m$, where $\rho = \Omega_n / \Omega$, $\Omega_n^2 = K_m / (1 + K_m)$ and A , B , α , β are constant. Hence, following the Krylov-Bogoliubov approach, one can try a first order approximation of the type $X_r = A(\theta)\cos[\rho\theta + \alpha(\theta)]$, $Y_r = B(\theta)\sin[\rho\theta + \beta(\theta)]$, $X_s = \Omega_n^2 X_r / K_m + a_s(\theta)$, $Y_s = \Omega_n^2 Y_r / K_m + b_s(\theta)$, imposing the additional conditions $X'_r = -\rho A(\theta)\sin[\rho\theta + \alpha(\theta)]$, $Y'_r = \rho B(\theta)\cos[\rho\theta + \beta(\theta)]$. Replacing this solution into Eqs. (17)

and neglecting terms of order ε^2 or smaller, two coupled differential systems are obtained for the six unknown functions $A(\theta)$, $B(\theta)$, $\alpha(\theta)$, $\beta(\theta)$, $a_s(\theta)$, $b_s(\theta)$:

$$\begin{aligned}
 A\alpha'\Omega_n\Omega\cos(\tau-\mu) + A'\Omega_n\Omega\sin(\tau-\mu) - K_m a_s &= \\
 &= \varepsilon \frac{\Omega_n^2}{K_m} A[\kappa\cos(\tau-\mu) - 2\delta\Omega_n\sin(\tau-\mu)] \\
 A\alpha'\Omega_n\Omega\cos(\tau-\mu) + A'\Omega_n\Omega\sin(\tau-\mu) + a_s &= \varepsilon\Phi_X
 \end{aligned}
 \tag{18a,b,c}$$

$$A\alpha'\sin(\tau-\mu) - A'\cos(\tau-\mu) = 0$$

$$\begin{aligned}
 B\beta'\Omega_n\Omega\sin(\tau+\mu) - B'\Omega_n\Omega\cos(\tau+\mu) - K_m b_s &= \\
 &= \varepsilon \frac{\Omega_n^2}{K_m} B[2\delta\Omega_n\cos(\tau+\mu) - \kappa\sin(\tau+\mu)] \\
 B\beta'\Omega_n\Omega\sin(\tau+\mu) - B'\Omega_n\Omega\cos(\tau+\mu) + b_s &= \varepsilon\Phi_Y
 \end{aligned}
 \tag{19a,b,c}$$

$$B\beta'\cos(\tau+\mu) + B'\sin(\tau+\mu) = 0$$

where it was put $\tau = \rho\theta + (\alpha + \beta)/2$ and $\mu = (\beta - \alpha)/2$ for brevity. Equations (18) and (19) indicate that the quantities A' , α' , a_s , B' , β' and b_s are small of order ε , whence the amplitudes $A(\theta)$ and $B(\theta)$ and the phases $\alpha(\theta)$ and $\beta(\theta)$ vary much more slowly than the argument $\rho\theta$.

Considering only the dominant terms of Φ_X and Φ_Y and carrying out some long calculations, we may arrive at

$$\begin{aligned}
 \Phi_X &= \left(\frac{d_{h,dry}}{d_{hi}} \right) \frac{B\sin(\tau+\mu) - A\rho\sin(\tau-\mu)}{\sqrt{W}\sqrt{1-k^2\sin^2(\tau-\phi)}} \\
 \Phi_Y &= \left(\frac{d_{h,dry}}{d_{hi}} \right) \frac{\rho B\cos(\tau+\mu) - A\cos(\tau-\mu)}{\sqrt{W}\sqrt{1-k^2\sin^2(\tau-\phi)}}
 \end{aligned}
 \tag{20a,b}$$

where $\tan 2\phi = [(A^2 + B^2)/(A^2 - B^2)] \times \tan 2\mu$, which relation is associated to the condition $(1 - \rho^2)\sin 2\mu / \sin 2\phi > 0$, and

$$\begin{aligned}
 W &= \frac{(A^2 + B^2)(1 + \rho^2) - 4AB\rho\cos 2\mu + |1 - \rho^2|\sqrt{A^4 + B^4 - 2A^2B^2\cos 4\mu}}{2} \\
 k^2 &= \frac{2|1 - \rho^2|\sqrt{A^4 + B^4 - 2A^2B^2\cos 4\mu}}{(A^2 + B^2)(1 + \rho^2) - 4AB\rho\cos 2\mu + |1 - \rho^2|\sqrt{A^4 + B^4 - 2A^2B^2\cos 4\mu}}
 \end{aligned}
 \tag{21a,b}$$

Moreover, neglecting the change of the slowly varying variables, the condition of equal dissipative work for dry and viscous friction reads

$$\frac{d_{h,dry}}{d_{h1}} = 2\Omega_n^2 \sqrt{W} \left\{ \frac{\int_0^{2\pi} [1 - k^2 \sin^2(\tau - \phi)] d\theta}{\int_0^{2\pi} \sqrt{1 - k^2 \sin^2(\tau - \phi)} d\theta} \right\} = \frac{\pi \Omega_n^2 \sqrt{W} \left(1 - \frac{k^2}{2}\right)}{E(k)} \quad (22)$$

where $E(k)$ is the Legendre's complete normal elliptic integral of the second kind.

Replacing Eqs. (20) into Eqs. (18-19), using Eqs. (21) and (22), solving for A' , B' , α' , β' , and integrating with respect to the "quick" variable τ over a period 2π , the slow gradients A' , α' , B' , β' turn out to be functions of the complete elliptic integrals of the first and second kinds, whose values may be found tabulated in several mathematical handbooks. Putting $\varepsilon_\Omega = \varepsilon / [\Omega_n(1+K_m)^2]$, $P = (2 - k^2)(K - E)/(k^2E)$, $Q = (2 - k^2)K/(2E)$, where $K(k)$ is the Legendre complete normal elliptic integral of the first kind, one gets

$$\begin{aligned} A' &= \varepsilon_\Omega \left\{ K_m^2 [(P - Q)B \cos 2\phi + QB \cos 2\mu - (P - Q)\rho A \cos 2(\mu - \phi) - \rho A Q] - \delta \Omega_n A \right\} \\ B' &= \varepsilon_\Omega \left\{ K_m^2 [-(P - Q)A \cos 2\phi + QA \cos 2\mu + (P - Q)\rho B \cos 2(\mu + \phi) - \rho B Q] - \delta \Omega_n B \right\} \\ A\alpha' &= \varepsilon_\Omega \left\{ K_m^2 [-(P - Q)B \sin 2\phi + QB \sin 2\mu - (P - Q)\rho A \sin 2(\mu - \phi)] + A\kappa/2 \right\} \\ B\beta' &= \varepsilon_\Omega \left\{ K_m^2 [(P - Q)A \sin 2\phi - QA \sin 2\mu - (P - Q)\rho B \sin 2(\mu + \phi)] - B\kappa/2 \right\} \end{aligned} \quad (23a,b,c,d)$$

Notice that, putting $P = Q = 1$, one regains the equations of the linear viscous case.

Multiplying Eq. (23a) by A , Eq. (23b) by B , minding the previous definition of ϕ and subtracting, one may arrive at the relation

$$\frac{(A^2 - B^2)'}{(A^2 - B^2)} = -2\varepsilon_\Omega \rho K_m^2 \left[\frac{\delta \Omega_n}{\rho K_m^2} + Q + (P - Q) \frac{\left(A^2 + B^2 - \frac{2AB \cos 2\mu}{\rho} \right) \operatorname{sgn}(1 - \rho^2)}{\sqrt{A^4 + B^4 - 2A^2 B^2 \cos 4\mu}} \right] \quad (24)$$

whose right hand turns out to be negative in the field of interest, so that $A - B \rightarrow 0$ and we may put $A \cong R$, $B \cong R$ after some time. Hence, putting $S = \sqrt{Q^2 + \rho^2(P - Q)^2}$, $\tan 2\psi = \rho(P - Q) \operatorname{sgn}(\sin 2\mu)/Q$, Eqs. (23 a,b) give place to

$$\frac{R'}{R} = \varepsilon_\Omega K_m^2 \left[S \cos 2(\mu + \psi) - \frac{\delta \Omega_n}{K_m^2} - Q\rho \right] \quad (25)$$

while Eqs. (23 c,d) give

$$(\mu + \psi)' = \frac{\beta' - \alpha'}{2} + \psi' = -\varepsilon_{\Omega} K_m^2 \left[S \sin 2(\mu + \psi) + \frac{\kappa}{2K_m^2} - (P - Q) \operatorname{sgn}(\sin 2\mu) \right] \quad (26)$$

P , Q , and S are very slowly varying functions of μ , A and B through the modulus k of the elliptic integrals and may be approximately considered invariant when integrating Eq. (26). Putting $b = \kappa / (2K_m^2) - (P - Q) \operatorname{sgn}(\sin 2\mu)$ for brevity. Equation (26) can be integrated to

$$\tan(\mu + \psi) = \frac{\sqrt{b^2 - S^2} \tan\left(-\varepsilon_{\Omega} K_m^2 \vartheta \sqrt{b^2 - S^2}\right) - S}{b} \quad \text{for } b^2 > S^2$$

$$\tan(\mu + \psi) = \frac{\left(\sqrt{S^2 - b^2} - S\right) \pm \left(\sqrt{S^2 - b^2} + S\right) \exp\left(-2\varepsilon_{\Omega} K_m^2 \vartheta \sqrt{S^2 - b^2}\right)}{b \left[1 \mp \exp\left(-2\varepsilon_{\Omega} K_m^2 \vartheta \sqrt{S^2 - b^2}\right)\right]} \quad (27 \text{ a,b})$$

for $b^2 < S^2$

where the upper sign holds for $b \tan(\mu + \psi) + S - \sqrt{S^2 - b^2} > 0$, the lower one vice versa and the new variable $\vartheta = \theta - \theta_0$ includes the integration constant θ_0 .

Equations (27 a,b) permit expressing $\cos 2(\mu + \psi)$ as a function of ϑ and integrating Eq. (25). Omitting the calculation procedure for brevity, it is possible to find that $\int_0^{\vartheta} [S \cos 2(\mu + \psi) - \delta \Omega_n / K_m^2 - \rho Q] d\vartheta$ is a diverging negative function of ϑ for $b^2 > S^2$, whereas for $b^2 < S^2$, it is easily observable that $\tan(\mu + \psi) \rightarrow -\left(S - \sqrt{S^2 - b^2}\right) / b$ for $\vartheta \rightarrow \infty$, implying that $\mu + \psi$ tends to an asymptotic nonzero value and $\cos 2(\mu + \psi) \rightarrow \pm \sqrt{1 - b^2 / S^2}$. Therefore, R tends to vanish and the motion is certainly stable for $b^2 > S^2$, whereas for $b^2 < S^2$, replacing the above asymptotic value of $\cos 2(\mu + \psi)$ into Eq. (25), it is possible to get the stability condition

$$\frac{\delta \Omega_n}{K_m^2} > \pm \sqrt{S - \left(\frac{\kappa}{2K_m^2}\right)^2 \left[1 - \left(\frac{2K_m^2}{\kappa}\right) (P - Q) \operatorname{sgn}(\sin 2\mu)\right]^2} - \rho Q \quad (28)$$

which, minding that $\Omega_n = \sqrt{K_m / (1 + K_m)}$, changes into Eq. (16) applying the "viscous values" $P = Q = S = 1$. Notice also that the condition $b^2 > S^2$ becomes $\kappa^2 / (4K_m^4) > 1$ in this case.

Equation (28) permits calculating the stability threshold levels of the external damping $\delta = d_{s,tot} / d_{h1}$ for the non-linear case, introducing suitable approximation formulas for the elliptic integrals, which give their values as functions of the square of the complementary modulus $m = 1 - k^2$ [25] and yield a precision of order 10^{-8} : $E(k) = 1 + \sum_{i=1 \text{ to } 4} (a_{Ei} - b_{Ei} \ln m) m^i$, $K(k) = 1 + \sum_{i=0 \text{ to } 4} (a_{Ki} - b_{Ki} \ln m) m^i$, where the coefficients are given by

Table 1. Coefficients of approximation formulas for complete elliptic integrals [25].

$a_{E1} = 0.44325141463$	$b_{E1} = 0.24998368310$
$a_{E2} = 0.06260601220$	$b_{E2} = 0.09200180037$
$a_{E3} = 0.04757383546$	$b_{E3} = 0.04069697526$
$a_{E4} = 0.01736506451$	$b_{E4} = 0.00526449639$
$a_{K0} = 1.38629436112$	$b_{K0} = 0.5$
$a_{K1} = 0.09666344259$	$b_{K1} = 0.12498593597$
$a_{K2} = 0.03590092383$	$b_{K2} = 0.06880248576$
$a_{K3} = 0.03742563713$	$b_{K3} = 0.03328355346$
$a_{K4} = 0.01451196212$	$b_{K4} = 0.00441787012$

Two indicative diagrams are reported as examples in Figs. 7 and 8, showing the threshold levels of the external dissipation needed to damp the whirl instability, for both the Coulombian and viscous models. As observable, the Krylov-Bogoliubov approach gives results in the non-linear case that are very close to the viscous assumption. Figure 7 shows the stability threshold in dependence on the shaft angular speed, for a fixed value of the anisotropy parameter of the suspension stiffness, and it is here to be remarked that negative threshold values indicate that there is no need of external dissipation sources (self-stabilizing rotor system). The plots of this first figure are monotonically increasing with the angular speed and thus, Figure 8 was traced, showing the stability threshold in dependence on the suspension anisotropy for infinite rotor speed, whose limit value indeed ensures the rotor stability throughout the whole speed range. It is observable that the increase of the suspension stiffness anisotropy yields a significant improvement of the stability conditions and, for anisotropy levels larger than a certain value, the rotor system turns out to be self-stabilizing for any angular speed, similarly to Fig. 5.

CONCLUSION

The present paper discusses on some procedures to counteract the destabilising effect of the shaft internal hysteresis in the supercritical regime of a rotating machine, by making use of external dissipative sources or by planning anisotropic support stiffness, differentiated in the horizontal and vertical planes. An equivalent coefficient of linear viscous damping, inversely proportional to the angular speed may be introduced for the calculation of the hysteretic friction force, which may be assumed proportional to the rotor centre velocity relative to a reference frame rotating with the shaft end sections. Otherwise, in the hypothesis of Coulombian internal friction, the internal force may be assumed constant and constantly in opposition to the relative velocity. The Routh-Hurwitz method may be applied to control the linear stability of the steady motion and the influence of several design characteristics of the rotor system on the stability may be analyzed, searching in particular for the viscous level needed for the stabilization in the whole speed range. The favourable effect of the support anisotropy is remarkable for symmetric rotors, but tends to become less efficacious when the rotor is mounted away from the mid-span. The two different hypotheses about the internal friction, viscous or dry, do not affect remarkably the

response and the stability of the rotating system, provided that the comparison is made in conditions of equal dissipative work in a sufficiently long run. Moreover, the simpler case of a symmetric rotor may be treated by averaging approximation techniques, e. g. of the Krylov-Bogoliubov type, capturing helpful formulas for the stability limits in correlation with the support stiffness characteristics.

REFERENCES

- [1] Montagnier, O., and Hochard, Ch., Dynamic instability of supercritical driveshafts mounted on dissipative supports—effects of viscous and hysteretic internal damping, *J. of Sound and Vibration*, v. 305, n. 3, pp. 378–400, (2007).
- [2] Sorge, F., Rotor whirl damping by dry friction suspension systems, *MECCANICA*, Springer, Vol. 43, n. 6, pp. 577-589, (2008).
- [3] Sorge, F., Damping of rotor conical whirl by asymmetric dry friction suspension, *Journal of Sound and Vibration*, Vol. 321, n. 1-2, pp. 79-103, (2009).
- [4] Sorge, F., and Cammalleri, M., Hysteretic whirl stabilization in rotor-shaft-bearing systems on dry friction suspension, XIX AIMETA National Congress, Ancona, Italy, 14-17 September 2009, cd-rom, (2009).
- [5] Sorge, F., and Cammalleri, M., Control of hysteretic instability in rotating machinery by elastic suspension systems subject to dry and viscous friction, *Journal of Sound and Vibration*, Vol. 329, n. 1-2, pp 1686-1701, (2010).
- [6] Newkirk, B.L., Shaft whipping, *General Electric Review*, Vol. 27, pp. 169-178 (1924).
- [7] Kimball, A.L., Internal friction theory of shaft whirling, *General Electric Review*, Vol. 27, pp. 244-251, (1924).
- [8] Robertson, D., Hysteretic influences on the whirling of rotors, *Proceedings of the Institute of Mechanical Engineers*, Vol. 131, pp. 513-537, (1935).
- [9] Gunter, E.J. jr., and Trumpler, P.R., The influence of internal friction on the stability of high speed rotors with anisotropic supports, *ASME Journal of Engineering for Industry*, Vol. 91, pp. 1105-1113, (1969).
- [10] Ryzhik, B., Sperling, L., and Duckstein, H., Auto-balancing of anisotropically supported rotors, *Technische Mechanik*, Band 24, Heft 1, pp. 37-50, (2004).
- [11] El-Marhomy, A.A., and Abdel-Sattar, N.E., Stability of rotor-bearing systems via Routh-Hurwitz criterion, *Applied Energy*, Vol. 77, pp. 287-308, (2004).
- [12] Penny, J.E.T., Friswell, M.I., Lees, A.W., and Garvey, S.D., A simple but versatile rotor model, 8th International Conference on Vibrations in Rotating Machinery, Swansea (UK), September 7-9, pp. 269-280, (2004).
- [13] Guo, Z., and Kirk, R.G., Theoretical study on instability boundary of rotor-hydrodynamic bearing systems: part I—Jeffcott rotor with external damping, *ASME Journal of Vibration and Acoustics*, Vol. 125, pp. 417-422, (2003).
- [14] Guo, Z., and Kirk, R.G., Theoretical study on instability boundary of rotor-hydrodynamic bearing systems: part II—rotor with external flexible damped support, *ASME Journal of Vibration and Acoustics*, Vol. 125, pp. 423-426, (2003).
- [15] Liu, L.X., and Spakovszky, Z.S., Effects of bearing stiffness anisotropy on hydrostatic micro gas journal bearing dynamic behavior, *ASME Journal of Engineering for Gas Turbines and Power*, Vol. 129, 177 (8 pages), (2007).

- [16] Panda, K.C., and Dutt, J.K., Design of optimum support parameters for minimum rotor response and maximum stability limit speed, *Journal of Sound and Vibration*, Vol. 223, n. 1, pp. 1-21, (1999).
- [17] Khulief, Y.A., and Mohiuddin, M.A., On the dynamic analysis of rotors using modal reduction, *Finite Element in Analysis and Design*, v. 26, pp. 41-55, (1997).
- [18] Genta, G., *Dynamics of Rotating Systems*, Springer, New York, U.S.A., pp. 227-263, (2005).
- [19] Rao, J.S., *Rotor Dynamics*, New Age Intern., New Delhi, 1996.
- [20] Childs, D., *Turbomachinery Rotordynamics*, J. Wiley & S., New York, 1993.
- [21] Sorge, F., and Cammalleri, M., An efficient damping technique for the unstable hysteretic rotor whirl by proper suspension systems, *ECOTRIB 2009*, Pisa, Italy, June 8-10, (2009).
- [22] Crandall, S.H., *Rotating and Reciprocating Machines*, *Handbook of Engineering Mechanics*, W. Flügge Editor, McGraw-Hill, New York, U.S.A., chapter 58, 13-24, (1962).
- [23] Wettergren, H.L., On the behavior of material damping due to multi-frequency excitation, *Journal of Sound and Vibration*, Vol. 206, n. 5, pp. 725-735, (1997).
- [24] Nayfeh, A.H., and Mook, D.T., *Nonlinear Oscillations*, Wiley, New York, U.S.A., (1979).
- [25] Abramowitz, M., and Stegun, I.A., *Handbook of Mathematical Functions with Formulas, Graphs and Mathematical Tables*, National Bureau of Standards, Applied Mathematical Series 55, U.S. Department of Commerce, (1964).

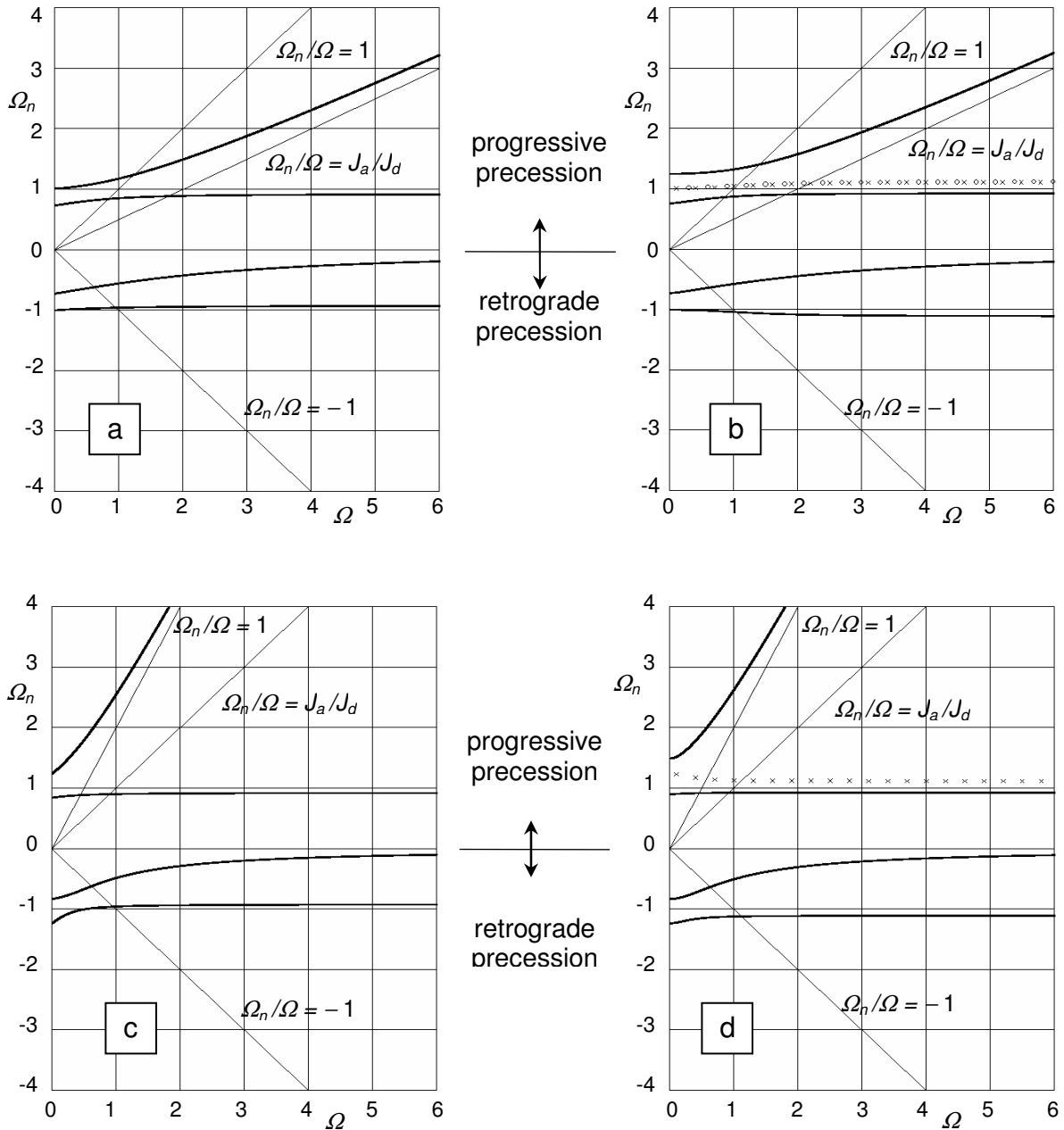


Fig. 2. Campbell diagrams $\Omega_n(\Omega)$ for $L_3 = 0.3$

(a) and (b): $J_a = 0.1, J_d = 0.2$ (oblong inertia ellipsoid)

(c) and (d): $J_a = 0.2, J_d = 0.1$ (oblate inertia ellipsoid)

(a) and (c): $K_{3x} = K_{4x} = 1, K_{3y} = K_{4y} = 1$

(b) and (d): $K_{3x} = K_{4x} = 1, K_{3y} = K_{4y} = 2$

Circles: axis whirl counter-directed. Crosses: front support whirl counter-directed

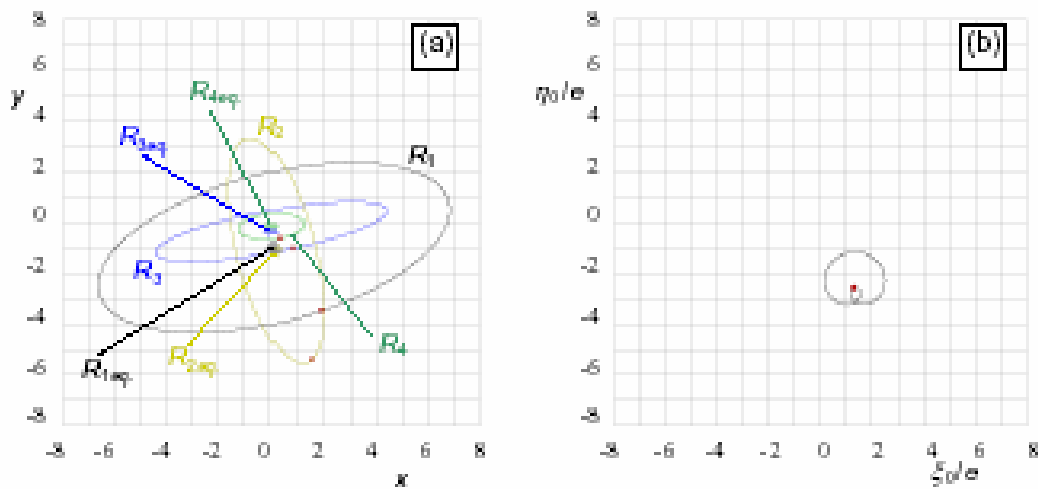


Fig. 3

(a) elliptical path of point O_1 ($R_1 = r_1/e$), of centres of back and front journal boxes ($R_3 = r_3/e$ and $R_4 = r_4/e$) and of rotor axis ($R_2 = l_s\sqrt{\varphi^2 + \psi^2}/e$), for $\Omega = 0.9$ (subscript eq. refers to equilibrium values, red circles refer to $\theta = 0$).

(b) double looped path of point O_1 in the rotating frame $O_3\xi_0\eta_0\zeta_0$ for $\Omega = 0.9$.

Data

$K_{3x} = K_{4x} = 1$, $K_{3y} = K_{4y} = 2$, $J_d = 0.1$, $J_a = 0.2$, $L_3 = 0.3$, $\Gamma = 1$, $M_d = 0.1$, $\gamma = 90^\circ$
 $d_1 = d_2 = 0.02$, $d_{3x} = d_{4x} = d_{3y} = d_{4y} = 0.1$, $d_{11} = 0.1$, $d_{12} = 0.05$.

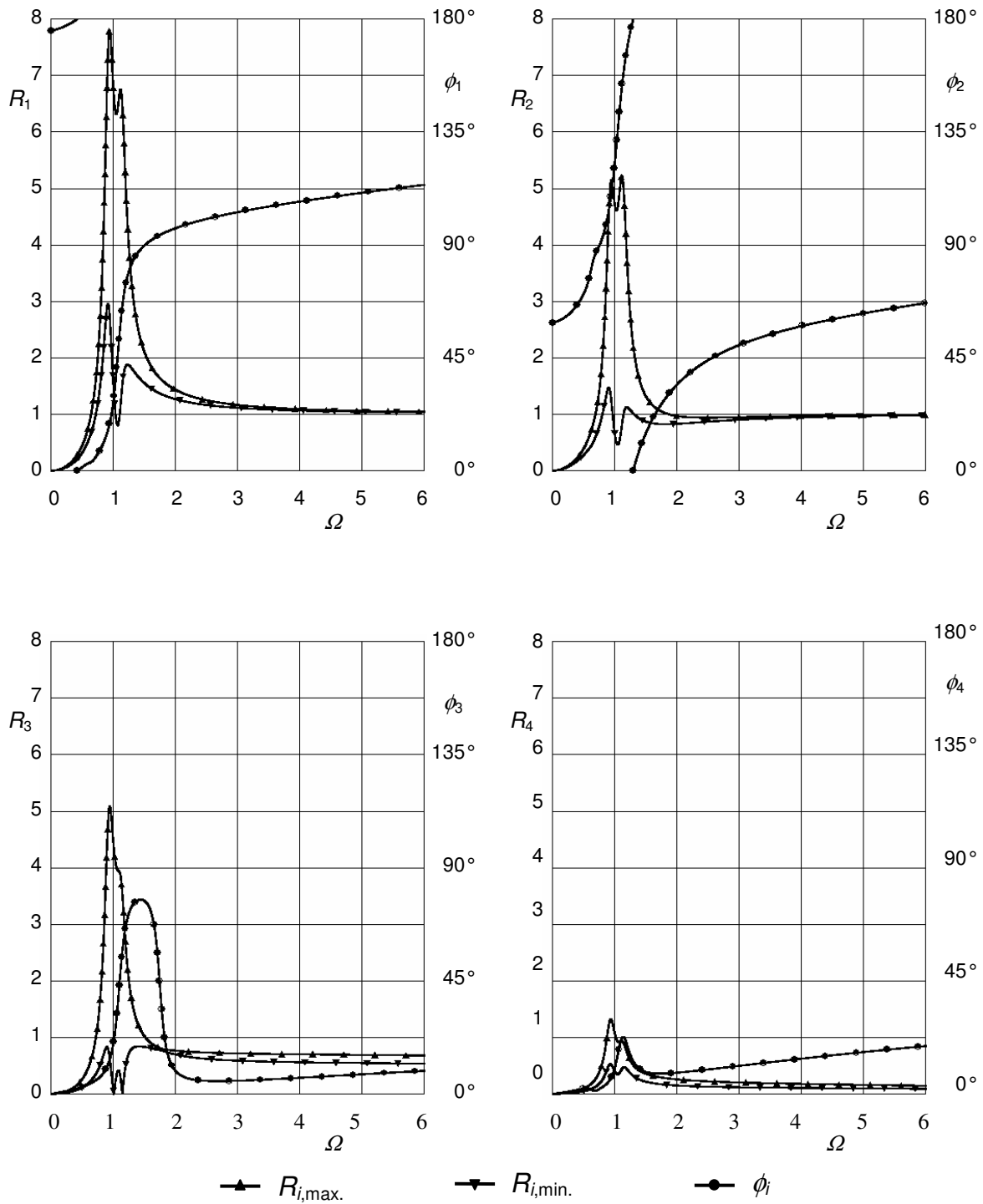


Fig. 4. Maximum and minimum orbital radii of the elliptical paths and slope of the principal axes vs rotor angular speed ($R_i = r_i/e$ for $i \neq 2$, $R_2 = l \sqrt{\varphi^2 + \psi^2} / e$).
 Data: $K_{3x} = K_{4x} = 1$, $K_{3y} = K_{4y} = 2$, $J_d = 0.1$, $J_a = 0.2$, $L_3 = 0.3$, $M_d = 0.1$, $\gamma = 90^\circ$
 $d_1 = d_2 = 0.02$, $d_{3x} = d_{4x} = d_{3y} = d_{4y} = 0.1$, $d_{h1} = 0.1$, $d_{h2} = 0.05$

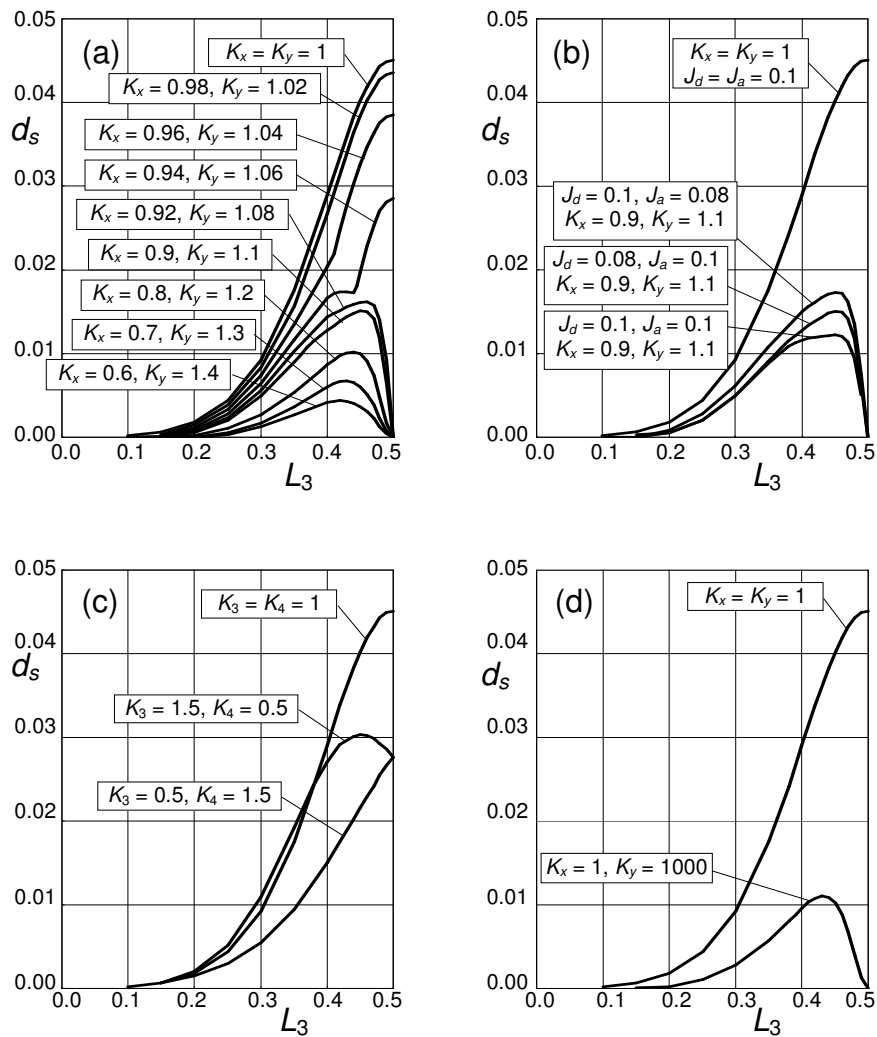


Fig. 5. Stability threshold d_s :

$$d_{3x} = d_{4x} = d_{3y} = d_{4y} = d_s, \quad d_1 = d_2 = 0, \quad d_{hi} = 0.02$$

- (a): influence of support anisotropy ($J_d = 0.08, J_a = 0.1, K_{3x} = K_{4x} = K_x, K_{3y} = K_{4y} = K_y$);
- (b): gyroscopic effect ($K_{3x} = K_{4x} = K_x, K_{3y} = K_{4y} = K_y$);
- (c): influence of support asymmetry ($J_d = 0.1, J_a = 0.1, K_{3x} = K_{3y} = K_3, K_{4x} = K_{4y} = K_4$);
- (d): comparison with "infinite" vertical stiffness ($J_d = 0.1, J_a = 0.1, K_{3x} = K_{4x} = K_x, K_{3y} = K_{4y} = K_y$)

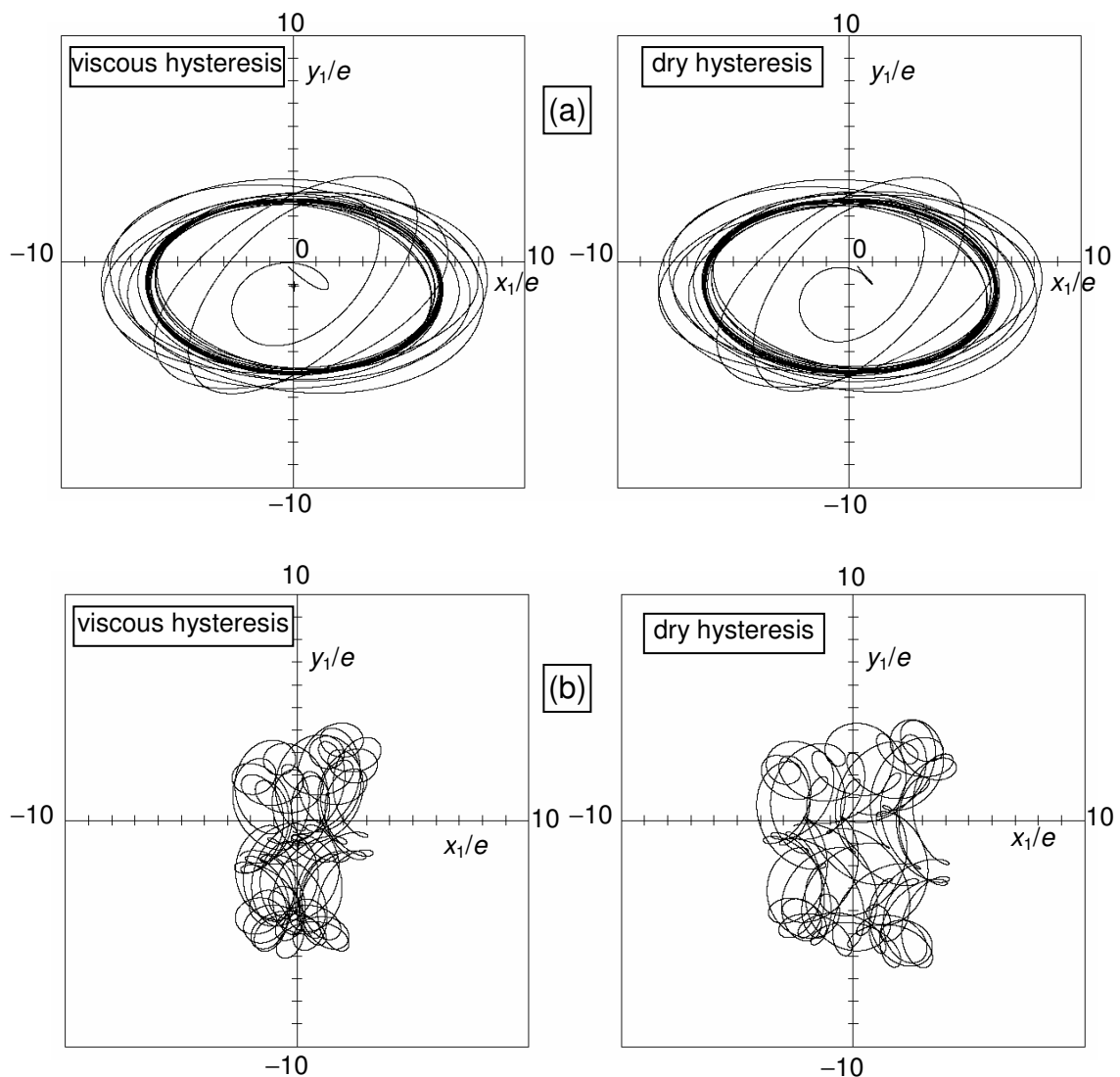


Fig. 6. Example of transient paths of point O_1 , for viscous and dry hysteretic force and equal dissipative work (50 revolutions). Data: $d_1 = d_2 = 0$, $d_h = 0.02$
 $K_{3x} = K_{4x} = 1$, $K_{3y} = K_{4y} = 3$, $J_d = 0.1$, $J_a = 0.2$, $L_3 = 0.4$, $\Gamma = 1$, $M_d = 1$, $\gamma = 90^\circ$
 (a): stable, $d_{3x} = d_{4x} = d_{3y} = d_{4y} = 0.1$, $d_{h,dry} = 0.049$, $\Omega = 0.8$
 (b): unstable, $d_{3x} = d_{4x} = d_{3y} = d_{4y} = 0.005$, $d_{h,dry} = 0.012$, $\Omega = 5$

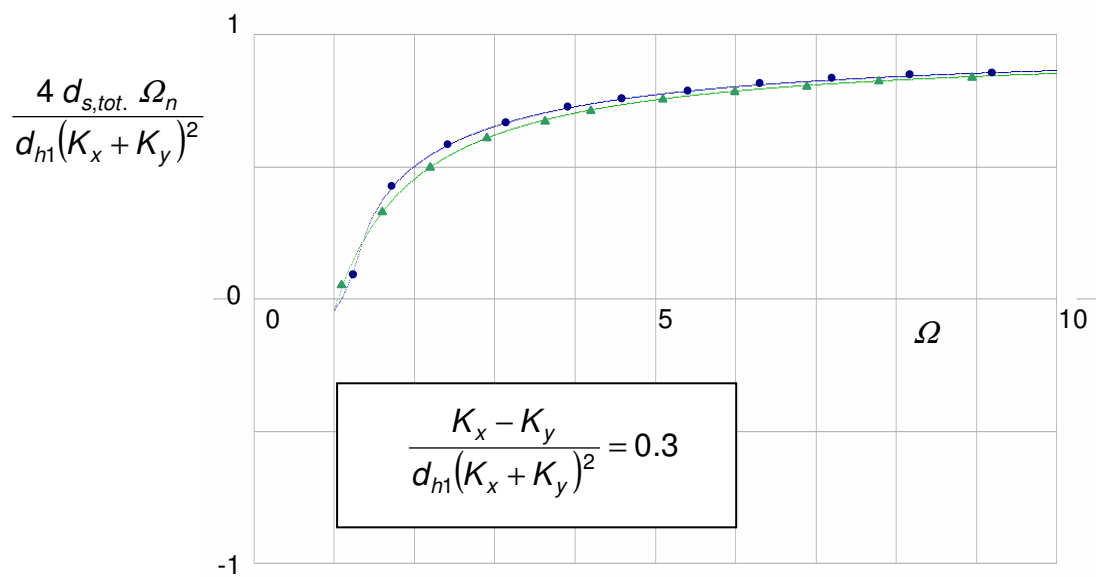


Fig. 7. Stability threshold of suspension-to-hysteretic damping ratio $d_{s,tot} / d_{h1}$ versus shaft angular speed, for fixed suspension anisotropy.
 K_x, K_y : dimensionless support stiffness coefficients in the horizontal and vertical directions.

—▲— viscous hysteresis

—●— Coulombian hysteresis

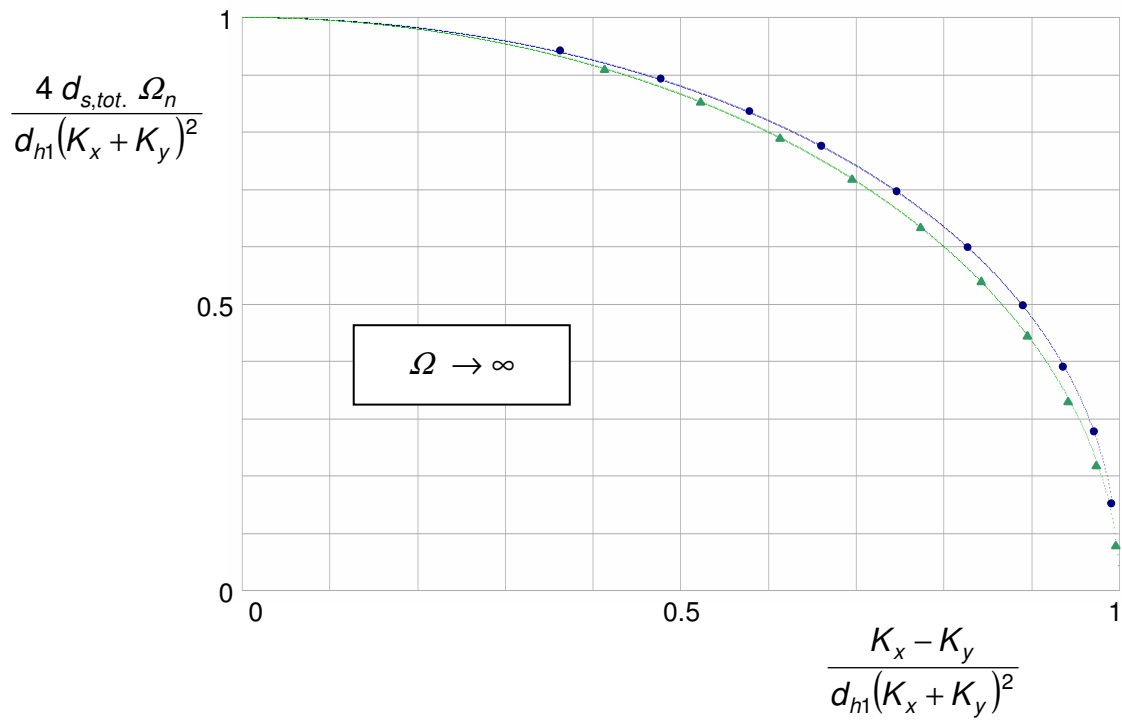


Fig. 8. Stability threshold of suspension-to-hysteretic damping ratio $d_{s,tot.} / d_{h1}$ versus support stiffness anisotropy, for infinite rotor angular speed. K_x, K_y : dimensionless support stiffness coefficients in the horizontal and vertical directions.

—▲— viscous hysteresis —●— Coulombian hysteresis